pISSN 1225-4339 eISSN 2287-4992
Korean J. Food Nutr. Vol. 35. No. 3, 178~184 (2022)
https://doi.org/10.9799/ksfan.2022.35.3.178

THE KOREAN JOURNAL OF
한국식품영양학회지
FOOD AND NUTRITION

[10]-Gingerol Induces Intrinsic Apoptosis in A2058 Human Melanoma Cells

Tae Eun Guon and †Ha Sook Chung*

Graduate Student, Dept. of Food and Nutrition, Duksung Women's University, Seoul 01369, Korea
**Professor, Dept. of Food and Nutrition, Duksung Women's University, Seoul 01369, Korea*

Abstract

The objective of the present study was to investigate the molecular mechanisms involved in the activity of [10]-gingerol using A2058 human melanoma cells. [10]-Gingerol inhibited the proliferation of A2058 cells by 50% at a concentration of 52 μM. Such inhibition was dose-dependent accompanied by morphological change indicative of apoptosis. Furthermore, flow cytometric analysis by Annexin V and PI double staining showed that [10]-gingerol increased the extent of apoptosis. Analysis of the mechanism of these events indicated that [10]-gingerol increased the ratio of Bax to Bcl-2, resulting in the activation of caspase-9, caspase-3, and poly-ADP-ribose polymerase in a dose-dependent manner.

Key words: [10]-gingerol, *Zingiber officinale* Roscoe, A2058, human melanoma cells, intrinsic apoptosis

Introduction

Melanoma is known to be one of the most malignant tumors, accounting for 65% of skin cancer deaths (Rigel & Carucci 2000). Exposure to direct or intermittent sunlight can increase the risk of melanoma (Cummins et al. 2006). Therefore, it is important to avoid direct UV exposure and to thoroughly apply sunscreen before UV exposure (Chen et al. 2008).

Apoptosis is involved in cell sculpture, tissue homeostasis, and the removal of unwanted cells. Cancer can be caused by the disruption of apoptotic regulation (Portt et al. 2011). The apoptotic mechanism is negatively regulated by the Bcl-2 family, which is the best mediator of apoptosis (Adams & Cory 1998). There is growing evidence regarding the role of the mitochondria in inducing apoptosis, resulting in the oligomerization and autoactivation of caspases (Green & Reed 1998). The pro-apoptotic member of the Bcl-2 family can directly signal the mitochondria to release cytochrome c (Park et al. 2013). In the early stages of apoptosis, pro-apoptotic signals activate separate signaling pathways via caspases (Igney & Krammer 2002; Martinvalet et al. 2005).

Ginger (*Zingiber officinale* Roscoe) is a commonly used tropical spice. It has pharmacological properties and is used to treat arthritis, aches, dementia, and hypertension. Despite the identification of more than 400 compounds, [6]-shogaol, [6]-gingerol, [8]-gingerol, and [10]-gingerol have been identified as major biologically active components responsible for gastroprotective, antihyperglycemic, antioxidant, antifungal, antiemetic, antipyretic, anti-cancer, and anti-inflammatory effects (Yoshikawa et al. 1993; Nakazawa & Ohsawa 2002; Ryu HS 2007; Ryu & Chung 2015; Guon & Chung 2016; Lee et al. 2020). It has been determined that the presence of α,β-unsaturated carbonyl groups is determined by the length of the carbon side chain, ultimately determining anti-oxidant and anti-inflammatory properties (Rolt & Cox 2020). Though there are currently convincing evidences on the anticancer effects of gingerols, it can be needed to determine the impact of gingerols on the molecular mechanism in A2058 human melanoma cells. In this study, we investigated the effects of [10]-gingerol on proliferation and apoptosis through activation of MAPK-mediated signaling, as well as alteration in Bcl-2 family protein expression and activation of caspase-9 and caspase-3 in A2058 cells. Interestingly, [10]-gingerol-mediated suppression of A2058 cells viability was significantly decreased in dose- and time dependent manners, which, in turn, led to caspase dependent signals.

† Corresponding author: Ha Sook Chung, Professor, Dept. of Food and Nutrition, Duksung Women's University, Seoul 01369, Korea. Tel: +82-2-901-8593, Fax: +82-2-901-8593, E-mail: hasook@duksung.ac.kr

Materials and Methods

1. Samples

Ginger (*Zingiber officinale* Roscoe) were purchased from NongHyup (Yangjae, Seoul), 2012. It was washed with bark and dried at room temperature for 2 days. The dried slices ginger (10 g) were extracted for 1 h, 3 times using 70% ethyl alcohol by maceration at 80℃. The extracted solution was filtered, concentrated and freeze-dried to produce yellowish powders (1.5635 g). (Guon & Chung 2016). Column chromatography was run on a silica gel 60 (70-230 mesh; Merck Millipore) and Sephadex LH-20 (25-100 mm; GE Healthcare Life Sciences, Uppsala, Sweden) eluting with *n*-hexane-ethyl acetate to yield [10]-gingerol. [10]-Gingerol was identified with co-TLC with references.

2. Materials

MTT, SP600125, PD98059, propidium iodide (PI) were purchased from Sigma-Aldrich (St. Louis, MO, USA). JNK, phopho-JNK, ERK, phopho-ERK, p38, phopho-p38, cleaved caspase-3, cleaved caspase-9, and PARP antibodies were purchased from Cell Signaling Technologies (Danvers, MA, USA). β-Actin, Bcl-2, Bax, and secondary antibodies, including goat anti-rabbit IgG-horseradish peroxidase and goat anti-mouse IgG, were purchased from Santa Cruz Biotechnology (Dallas, TX, USA). The chemicals and instruments used in the experiments were prepared according to previously described methods (Ryu & Chung 2015; Guon & Chung 2016).

3. Cell culture and cell viability assay

A2058 and HaCaT cells were purchased from American Type Culture Collection. The cells were maintained in DMEM supplemented with 100 units/mL penicillin, 10% FBS, and 100 μg/mL streptomycin at 37℃ under 5% CO_2 atmosphere. Cell counts were performed using a hemocytometer. [10]-Gingerol was dissolved in DMSO and directly applied to the culture medium. The cytotoxicity of [10]-gingerol (Fig. 1) was estimated colorimetrically (Carmichael et al. 1987; Ryu & Chung 2016). The absorbance of the supernatant was estimated spectrophotometrically at 540 nm. The results are presented as the mean±standard deviation (SD) of at least three trials.

4. Nuclear staining with Hoechst 33258

A2058 cells were treated 10, 25, and 50 μM [10]-gingerol;

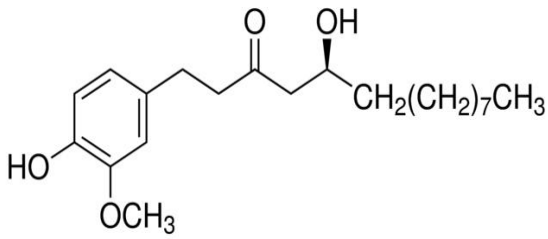

Fig. 1. Chemical structure of [10]-gingerol.

fixed for 30 min at 37℃ in 100% methanol; washed with PBS; and stained with Hoechst 33258 (2 μg/mL) (Ryu & Chung 2016). Apoptotic cells were observed using a BX51 fluorescence microscope with a DP70 camera (Olympus Corporation, Tokyo, Japan). The nuclear morphology of the cells was observed using DNA-specific blue fluorescent dye Hoechst 33258. The viable cells were stained homogeneously, whereas the apoptotic cells that had shown chromatin condensation or nuclear fragmentation were not stained.

5. Apoptosis analysis

Annexin V/PI double staining assay was carried out to further differentiate early and late apoptosis stages. The assay was determined using an *ApoScan*™ Annexin V-FITC apoptosis detection Kit (BioBud Co. Ltd., Seoul, Korea) in [10]-gingerol-treated with PBS. The cells were trypsinized, harvested, and washed with PBS, and then cells were resuspended in 1×binding buffer (500 μL) and incubated with 1.25 μL of Annexin V-FITC (200 μg/mL) at room temperature for 15 min. The supernatant was then removed after centrifugation at 400 ×g at 4℃ for 10 min. The cells were then resuspended in 500 μL of 1×binding buffer, and cell suspensions were then stained with 10 μL of PI (30 μg/mL) at 4℃ in the dark. Fluorescence was quantified using FACSCalibur flow cytometry (Becton Dickinson & Com., San Jose, CA). The amounts of cells in early and late apoptosis was determined as the percentage of Annexin V+/PI− or Annexin V+/PI+ cells, respectively.

6. Western blotting analysis

Protein extraction and western blot analysis were performed as described previously (Ryu & Chung 2016). The cultured cells were harvested, lysed, and then centrifuged at 13,000 ×g for 15 min. The lysates were mixed with 5× sample buffer and heated to 95℃ for 5 min. Equal amounts of protein were separated by 12% SDS-PAGE and transferred onto nitrocellulose membranes.

The membranes were washed, and protein bands were detected using an enhanced chemiluminescence western blotting detection kit (Bio-Rad Laboratories, Inc., Hercules, CA, USA). β-Actin, TBP, and specific protein levels are presented as the fold change relative to the control. Densitometry was performed using Image J software (National Institutes of Health, Bethesda, MD, USA).

7. Statistical analysis

SPSS software version 22.0 (IBM SPSS, Armonk, NY, USA) was used to analyze the data. Significance was determined one-way ANOVA with Tukey's test. *P*-value<0.05 was considered to indicate a statistically significant difference.

Results and Discussion

1. Inhibitory effects of [10]-gingerol in A2058 cells

In the present study, we examined the effects of [10]-gingerol on the growth of A2058 human melanoma cells by the MTT assay. Cells were exposed to various concentrations (0~100 μM) of [10]-gingerol and their viability was determined. Cytotoxicity was determined as the percentage of viable treated cells in comparison with viable cells of untreated control cells. As shown in Fig. 2A, [10]-gingerol significantly inhibited the proliferation of A2058 cells in a dose-dependent manner. Treatment with [10]-gingerol for 72 h with concentrations of 10, 25, 50, 75, and 100 μM decreased the viability of A2058 cells by 81.1%, 74.1%, 48.7%, 44.8%, and 42.9%, respectively with IC_{50} values of 52 μM. To determine whether [10]-gingerol can induce cytotoxicity in normal human keratinocytes (HaCaT) cells, MTT assay also achieved (Fig. 2B). HaCaT cells were found to be more resistant to A2058 cells treated with [10]-gingerol. Therefore, [10]-gingerol concentrations of 10, 25, and 50 μM were used for the subsequent experiments in A2058 cells.

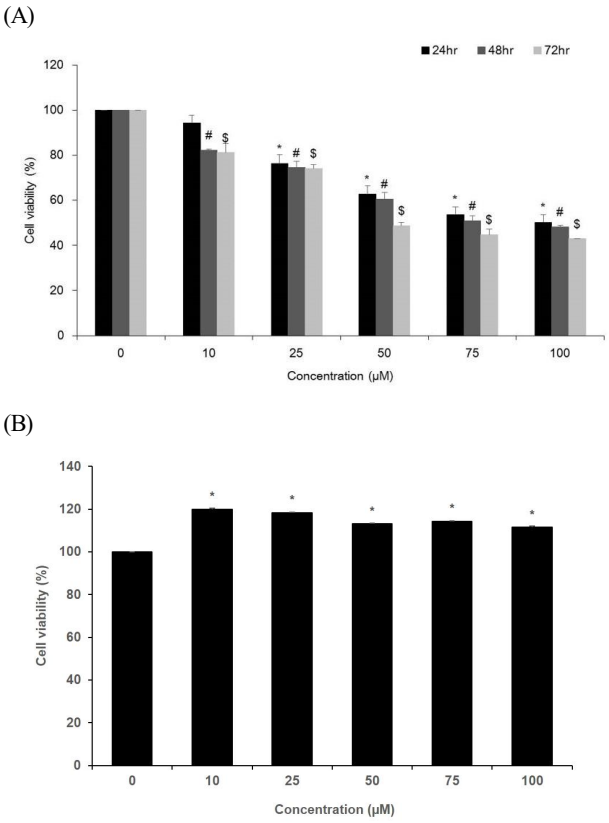

Fig. 2. Cytotoxic effect of [10]-gingerol. (A) Cytotoxic effects of 10-gingerol in A2058 cells in time and dose dependent manners. After treatment with [10]-gingerol for 24, 48, and 72 hr. Each bar indicated the mean±standard deviation (SD, $^{*}p$<0.05, significantly different from control cells for 24 hr; $^{\#}p$<0.05, significantly different from control cells for 48 hr; $^{\$}p$<0.05, significantly different from control cells for 72 hr). (B) Cytotoxic effects of [10]-gingerol in HaCaT human keraninocytes in a dose dependent manner. After treatment with [10]-gingerol for 72 hr. Each bar indicated the mean±standard deviation (SD, $^{*}p$<0.05, significantly different from control cells).

2. Induction of apoptosis by [10]-gingerol in A2058 cells

Apoptosis is commonly known as physiological programmed cell death and is characterized by a series of morphological hallmarks (Kumar et al. 2010). In order to determine whether [10]-gingerol-induced growth inhibition in A2058 cells was associated with the induction of apoptosis, DNA-binding dye Hoechst 33258 staining was performed. As shown in Fig. 3, the nuclei showed homogeneously stained and an intact structure in control cells. After the treatment of [10]-gingerol, there was the induction of apoptosis by morphological changes on A2058 cells. The population of live cells dropped slightly, and the morphology of the cells changed with reduction in the cell volume (pyknosis) with [10]-gingerol. Treatment with 10 μM [10]-gingerol resulted in slight cell shrinkage and reduction of cell numbers. However, increasing the [10]-gingerol dose to 25 and 50 μM, resulted in marked apoptotic morphological alterations, including membrane blebbing, nuclear fragmentation, chromatin condensation, and increased fluorescent intensity. In particular, crescent-shaped nuclei, a typical characteristic of apoptotic cells, were observed at 50 μM [10]-gingerol treatment.

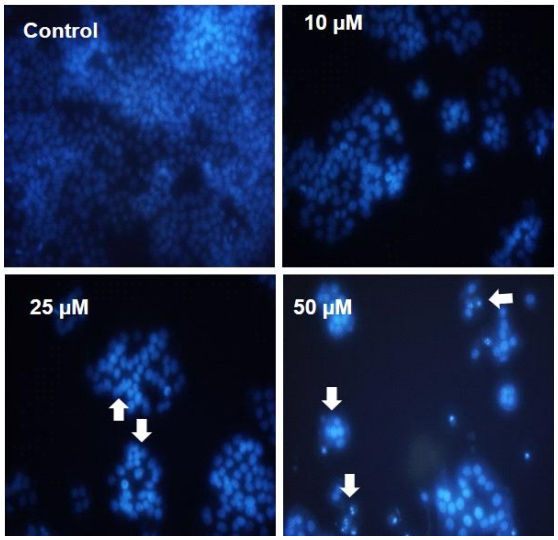

Fig. 3. Microscopy image of [10]-gingerol-treated A2058 cells in a dose dependent manner. After incubation with 0, 10, 25, and 50 μM [10]-gingerol for 72 hr, the cells were observed by fluorescent microscopy using Hoechst 33258 staining (arrow indicates the formation of apoptotic bodies).

At a higher [10]-gingerol dose of 50 μM, these characteristics were even more evident and the cells exhibited partial detachment. These results suggest that [10]-gingerol exerts antiproliferative activities in a dose-dependent manner, and is consistent with MTT results.

3. Effects of [10]-gingerol on apoptosis in A2058 cells

To further investigated the apoptotic cells, Annexin V and PI double staining were used and were analyzed by flow cytometry analysis. Annexin V－PI－ and Annexin V+PI+ populations represent viable and late apoptotic cells, respectively. Apoptotic populations were increased in A2058 cells treated with [10]-gingerol (Fig. 4A). Treatment with 10, 25, and 50 μM [10]-gingerol increased the number of early apoptotic cells by 9.2%, 13.5%, and 29.5%, respectively, compared to the control (2.2%). Moreover, treatment with 10, 25, and 50 μM [10]-gingerol increased the number of late apoptotic cells by 9.9%, 13.3%, and 28.1%, respectively, compared to the control (4.5%). Treatment with 10, 25, and 50 μM [10]-gingerol increased the number of total apoptotic cells by 19.0%, 26.8%, and 42.4%, respectively (Fig. 4B). The increase in the number of early apoptotic cells was greater than that in the number of late apoptotic cells on treatment with 25 and 50 μM [10]-gingerol. In the early stages of apoptosis, PS is exposed on the external

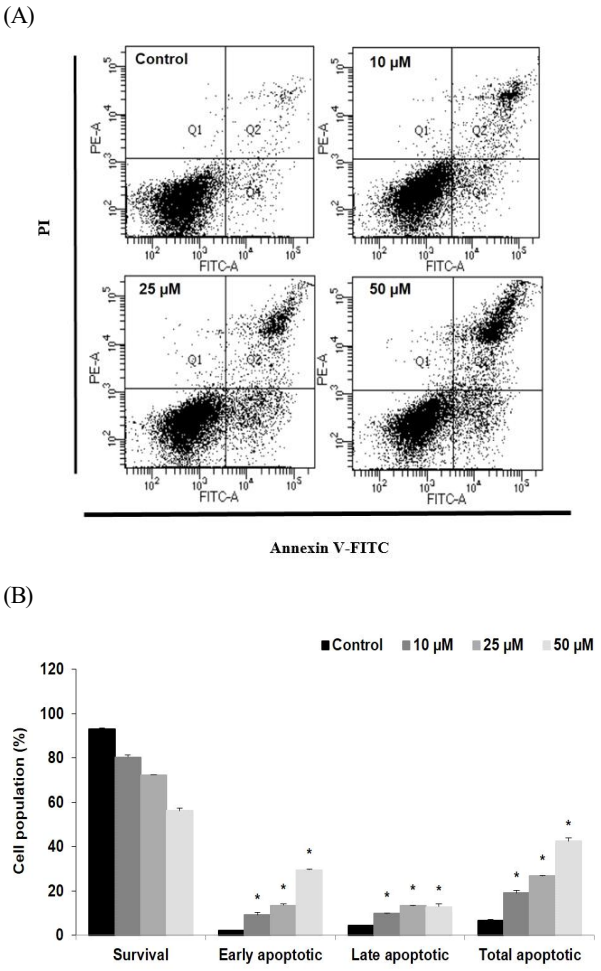

Fig. 4. Effects of [10]-gingerol on apoptosis in A2058 cells in a dose dependent manner. (A) Flow cytometric analysis of A2058 cells incubated with [10]-gingerol for 72 hr. The right bottom quadrant represents Annexin V-stained cells (early-phase apoptotic cells). The top right quadrant represents PI－ and Annexin V-stained cells (late-phase apoptotic cells). (B) Statistical analysis of apoptosis. $^{*}p<0.05$, significantly different from control cells.

cell surface (Lee et al. 2013). Anti-apoptotic proteins prevent apoptosis by blocking the release of cytochrome c from the mitochondria. Pro-apoptotic proteins are regulated by promoting such release. These results present [10]-gingerol induced anti-proliferative activities against A2058 cells, which were caused by inducing apoptosis in a dose-dependent fashion.

4. Effects of [10]-gingerol on the expression of Bcl-2 family and caspase protein

Caspases, a family of cysteine proteases, play essential roles

in intracellular protein cleavage by signaling apoptosis. The intrinsic apoptosis pathway is controlled by the Bcl-2 family, which prevents mitochondrial permeability transition pores from opening during apoptosis (Armstrong JS 2007). Bcl-2 interacts with the mitochondrial plasma membrane and prevents mitochondrial membrane pores from opening during apoptosis, blocking the signals of apoptotic factors, such as Bax (Ryu et al. 2013). The A2058 melanoma cells exposed to [10]-gingerol showed a concentration-dependent reduction in the level of Bcl-2 protein, with a concomitant increase in the level of Bax. With the change of Bcl-2 family proteins, the activation of caspase-9 and caspase-3, an effective caspase, was accompanied (Figs. 5A, 5B). Moreover, poly ADP-ribose polymerase (PARP) cleavage, an indicator of apoptosis, was also elevated (Fig. 5C). The mitochondrial-related pathway is regulated by anti-apoptotic (Bcl-2, Bcl-x, and Bcl-XL) and pro-apoptotic members (Bax, Bak, Bid, Bad, and Bim) of the Bcl-2 family (Liu et al. 2016). Cell death signals cause the release of cytochrome c from the mitochondria and activate caspase-9 in this pathway (Araya et al. 2021). Caspase-3 cleaves most cellular substrates in apoptotic cells. It is activated following cleavage by caspase-9 (Pereira & Song 2008). At present, apoptotic signals involve two main pathways: the extrinsic or death receptor pathway and the intrinsic or mitochondrial-mediated pathway (Pfeffer & Singh 2018). These results presented that [10]-gingerol can lead to apoptosis by caspase-related protein family and might be through intrinsic mitochondrial apoptosis pathway.

5. Effects of [10]-gingerol on the expression of MAPK

Mitogen-activated protein kinases (MAPKs) signaling cascades, including c-Jun amino-terminal kinases (JNKs), extracellular signal-regulated kinases (ERKs), and p38 kinase, are found in all eukaryotes and play a central role in regulating cell proliferation, differentiation and apoptosis (Kim & Choi 2015). As shown in Fig. 6A, the levels of p-ERKs, p-JNKs, and p-p38 MAPKs were significantly elevated on treatment with [10]-gingerol for 24 h. In contrast, the levels of non-phosphorylated JNKs, ERKs, and p38 MAPKs remained unchanged. Thus, 50 μM [10]-gingerol caused apoptosis through ERKs, JNKs, and p38 MAPKs in A2058 cells. To further determine whether JNK, ERK and p38 are involved in the [10]-gingerol-induced A2058 cytotoxicity, the kinase-specific inhibitors, SP600125, PD98059, or SB203580, were incubated. As shown in Fig. 6B, the p-JNK levels decreased on co-treatment with SP600125 and [10]-gingerol. Similarly,

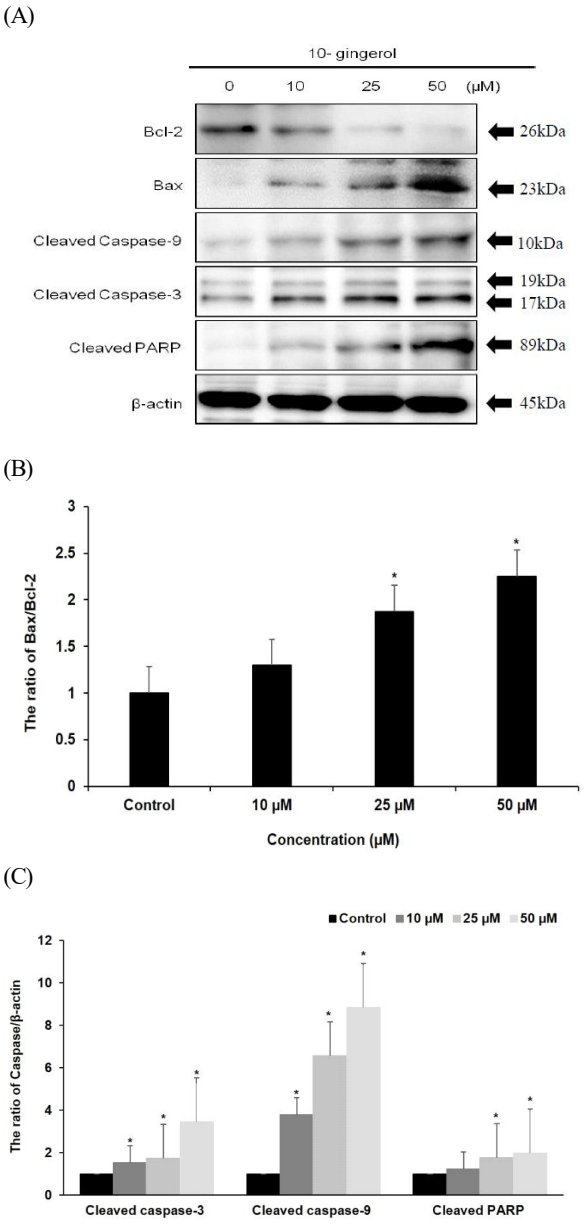

Fig. 5. Effects of [10]-gingerol on the expression of Bcl-2 family and caspase-related proteins in A2058 cells in a dose dependent manner. (A) Cells were treated with 0, 10, 25, and 50 μM [10]-gingerol for 72 hr. The cell lysates were electrophoresed and western blotting with Bcl-2, Bax, caspase-9, caspase-3, and cleaved PARP antibodies. (B) Effects of [10]-gingerol on the expression of Bcl-2 family related protein in A2058 cells from statistical analysis. $^{*}p<0.05$, significantly different from control cells in intact cells. (C) Effects of [10]-gingerol on the expression of caspase-related proteins in A2058 cells. $^{*}p<0.05$, significantly different from control cells in intact cells.

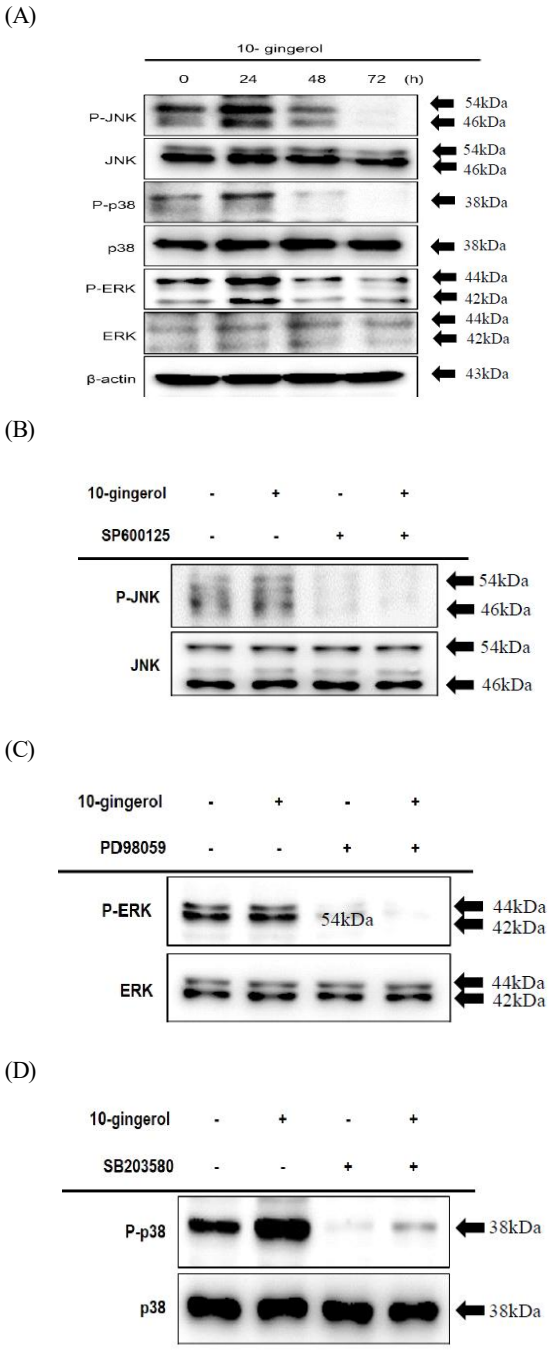

Fig. 6. Regulation of MAPKs in [10]-gingerol-treated A2058 cells in a time dependent manner. (A) An equal amount of cell lysates electrophoresed and ERK, JNK, p38, and their phosphorylated expression form were detected by western blotting analysis with corresponding antibodies. (B) Role of JNK in [10]-gingerol-induced apoptosis in A2058 cells. (C) Role of ERK in [10]-gingerol-induced apoptosis in A2058 cells. (D) Role of p38 in [10]-gingerol-induced apoptosis in A2058 cells.

co-treatment with PD98059, SB203580, [10]-gingerol effectively inhibited p-ERK and p38 MAPK upregulation (Figs. 6C, 6D). These cumulative results suggest that JNKs, ERKs, and p38 MAPKs are involved in [10]-gingerol-induced intrinsic pathway.

Conclusion

In the present study, we investigated apoptosis in A2058 human melanoma cells which were treated with various concentrations of [10]-gingerol (0-100 μM). [10]-Gingerol suppressed the growth of A2058 cells in dose- and time-dependent manners. This effect appeared that [10]-gingerol to be mediated by the induction of apoptosis, as evidenced by morphological changes, cell shrinkage, condensed chromatin, and the formation of apoptotic bodies via staining with the DNA-binding dye Hoechst 33258. [10]-Gingerol increased Bax expression but decreased the expression of Bcl-2, each in a dose-dependent manner. The mitochondrial plasma membrane disruption by [10]-gingerol was followed by the activation of caspase-9, caspase-3, and its target, PARP. Western blotting experiments indicated that caspase-9 and caspase-3 appear to be activated in [10]-gingerol-induced A2058 cells. The cleaved form of PAPR was also detected in [10]-gingerol treated A2058 cells. And the phosphorylated JNK and ERK, and p-38 significantly blocked in response to co-treatment with [10]-gingerol and SP600125, PD98059, or SB203580, respectively. These data indicate that [10]-gingerol induced apoptosis via the intrinsic pathway.

References

Adams JM, Cory S. 1998. The Bcl-2 protein family: Arbiters of cell survival. *Science* 281:1322-1326

Araya LE, Soni IV, Hardy JA, Julien O. 2021. Deorphanizing caspase-3 and caspase-9 substrates in and out of apoptosis with deep substrate profiling. *ACS Chem Biol* 16:2280-2296

Armstrong JS. 2007. Mitochondrial medicine: Pharmacological targeting of mitochondria in disease. *Br J Pharmacol* 151: 1154-1165

Carmichael J, DeGraff WG, Gazdar AF, Minna JD, Mitchell JB. 1987. Evaluation of a tetrazolium-based semiautomated colorimetric assay: Assessment of chemosensitivity testing. *Cancer Res* 47:936-942

Chen J, He X, Peng H, Ou-Yang X, He X. 2008. Research on the antitumor effect of ginsenoside Rg3 in B16 melanoma

cells. *Melanoma Res* 18:322-329

Cummins DL, Cummins JM, Pantle H, Silverman MA, Leonard AL, Chanmugam A. 2006. Cutaneous malignant melanoma. *Mayo Clin Proc* 81:500-507

Green DR, Reed JC. 1998. Mitochondria and apoptosis. *Science* 281:1309-1312

Guon TE, Chung HS. 2016. Effect of *Zingiber officinale* Roscoe extract on antioxidant and apoptosis in A2058 human melanoma cells. *J East Asian Soc Diet Life* 26:207-214

Igney FH, Krammer PH. 2002. Death and anti-death: Tumour resistance to apoptosis. *Nat Rev Cancer* 2:277-288

Kim EK, Choi EJ. 2015. Compromised MAPK signaling in human diseases: an update. *Arch Toxicol* 89:867-882

Kumar V, Abbas AK, Fausto N, Aster JC. 2010. Robins and Cotran: Pathologic Basis and Disease. 8th ed. p.25. Saunders

Lee KH, Shin ES, Sim EJ, Bae YJ. 2020. Comparison of antioxidant and antimicrobial activities of fingerroot (*Boesenbergia pandura*) and ginger (*Zingiber officinale* Roscoe). *Korean J Food Nutr* 33:105-110

Lee SH, Meng XW, Flatten KS, Loegering DA, Kaufmann SH. 2013. Phosphatidylserine exposure during apoptosis reflects bidirectional trafficking between plasma membrane and cytoplasm. *Cell Death Differ* 20:64-76

Liu JF, Chen CY, Chen HT, Chang CS, Tang CH. 2016. BL-038, a benzofuran derivative, induces cell apoptosis in human chondrosarcoma cells through reactive oxygen species/ mitochondrial dysfunction and the caspases dependent pathway. *Int J Mol Sci* 17:1491

Martinvalet D, Zhu P, Lieberman J. 2005. Granzyme A induces caspase-independent mitochondrial damage, a required first step for apoptosis. *Immunity* 22:355-370

Nakazawa T, Ohsawa K. 2002. Metabolism of [6]-gingerol in rats. *Life Sci* 70:2165-2175

Park HY, Kim GY, Kwon TK, Hwang HJ, Kim ND, Yoo YH, Choi YH. 2013. Apoptosis induction of human leukemia U937 cells by 7,8-dihydroxyflavone hydrate through modulation of the Bcl-2 family of proteins and the MAPKs signaling pathway. *Mutat Res Genet Toxicol Environ Mutagen* 751:101-108

Pereira NA, Song Z. 2008. Some commonly used caspase substrates and inhibitors lack the specificity required to monitor individual caspase activity. *Biochem Biophys Res Commun* 377:873-877

Pfeffer CM, Singh ATK. 2018. Apoptosis: A target for anticancer therapy. *Int J Mol Sci* 19:448

Portt L, Norman G, Clapp C, Greenwood M, Greenwood MT. 2011. Anti-apoptosis and cell survival: A review. *Biochim Biophys Acta Mol Cell Res* 1813:238-259

Rigel DS, Carucci JA. 2000. Malignant melanoma: Prevention, early detection, and treatment in the 21st century. *CA Cancer J Clin* 50:215-236

Rolt A, Cox LS. 2020. Structural basis of the anti-ageing effects of polyphenolics: Mitigation of oxidative stress. *BMC Chem* 14:50

Ryu HS. 2007. The effects of *Zingiber officinale* Roscoe extracts on mouse IFN-r and IL-10 production. *Korean J Food Nutr* 20:259-264

Ryu MJ, Kim AD, Kang KA, Chung HS, Kim HS, Suh IS, Chang WY, Hyun JW. 2013. The green algae *Ulva fasciata* Delile extract induces apoptotic cell death in human colon cancer cells. *In Vitro Cell Dev Biol Anim* 49:74-81

Ryu MJ, Chung HS. 2015. [10]-Gingerol induces mitochondrial apoptosis through activation of MAPK pathway in HCT116 human colon cancer cells. *In Vitro Cell Dev Biol Anim* 51:92-101

Ryu MJ, Chung HS. 2016. Fucoidan reduces oxidative stress by regulating the gene expression of HO-1 and SOD-1 through the Nrf2/ERK signaling pathway in HaCaT cells. *Mol Med Rep* 14:3255-3260

Yoshikawa M, Hatakeyama S, Chatani N, Nishino Y, Yamahara J. 1993. Qualitative and quantitative analysis of bioactive principles in *Zingiberis rhizoma* by means of high performance liquid chromatography and gas liquid chromatography. On the evaluation of *Zingiberis rhizoma* and chemical change of constituents during *Zingiberis rhizoma* processing. *Yakugaku Zasshi* 113:307-315

Received 08 April, 2022
Revised 18 April, 2022
Accepted 10 May, 2022